Mapping Rice by growth stage using POLSAR: preliminary results from the Philippines.

Hugh Turral[1]

Background

Rice is the most important irrigated crop in SE Asia, but it is hard to ascertain exact areas because:

- There is no distinct crop season in the tropics. Where water is available, rice can grow all year round, and due to labour and other constraints in the sequence of agricultural operations, it is normal to find that there is a lot of spatial variability at medium and local scales in crop growth stages.
- Even where crop seasons are more pronounced (North Vietnam, central Luzon, and in the Yangtze River Basin (PRC), there can be a long periods of planting and harvest. In the Red River Delta, rice is transplanted over a two-month window. If there is a need for replanting (due to frost in Spring or flooding in summer), the time between first and last planting can be as much as 90 days, or the entire duration of a short season variety.

There is a lack of planning and coordination between farmers, irrigation suppliers and agricultural services in rice planting. This results in considerable local-scale and service area variability in planting patterns and coverage, and uncertain stagger and spread of the planting window in seasonal areas.

The improvement of irrigation system performance includes the timely delivery of the correct quantities of water to the right place to satisfy crop water requirements (evapotranspiration and additionally soil saturation for rice). Computer simulation models can be applied to compute the amount of evapotranspiration, and accumulate water deliveries through the irrigation network to determine releases at the head of the system – for example a dam or a pumping station (FAO, 1996). Correct quantification of water requirements is dependent on knowledge of the crop area, crop type and growth stage.

Growth stage may be inferred from date of planting and crop characteristics. In practice, it is rare that either is known with any accuracy. In tropical situations, such as southern Vietnam and Indonesia, rice may be grown continuously with as many as 7 short duration crops in two years. In such situations, it is common to find rice at all growth stages simultaneously in any given area. In Dutch colonial Indonesia, crop areas were surveyed every 10 days, using cadastral maps, but such practices are no longer economically or logistically possible.

Remote sensing offers good opportunities for crop identification and classification, and has become a mature and useful technology using visual band /NIR/TIR imagery.

[1] International Development Technologies Centre, University of Melbourne, Australia. Now at the International Water Management Institute, Colombo, Sri Lanka. h.turral@cgiar.org

However, in the tropics and sub-tropics, cloud cover prevents the timely acquisition of such imagery, and in Hanoi (N. Vietnam) there are on average less than 60 cloud free days per year.

Single band Synthetic Aperture Radar sensors (ERS-1 and 2, Radarsat) have been used to map rice in Indonesia and in the Mekong region (Radarsat International, pers. comm. 2000), but require multi-temporal image analysis, based on threshold changes in backscatter (Le Toan, 1997) to differentiate rice from other crops and from ponds, fallow and bare land etc. Classification accuracy is not good, especially as prior knowledge of planting date is required for multi-temporal analysis, and is in fact rarely known as previously explained.

Single band, single polarization data offers very limited possibilities for crop discrimination at one time of acquisition, but there are much greater possibilities with multi-polar, multi-band sensors such as AIRSAR.

The ultimate objective of the research is to develop the simplest possible robust crop identification scheme that distinguishes rice by its growth stage in order to provide real-time rice maps for use in irrigation system management. The short term objective is to use the power and sophistication of POLSAR to test mapping schemes using different combinations of band and polarization, and derived data such as texture, band ratios, phase images and bounce images.

The investigation of SAR for rice mapping was developed as part of an ACIAR[2] funded project "System wide water management in public irrigation systems in Vietnam". Ground truth data were due to be collected at the Cu Chi irrigation system, 40 km NW of Saigon, in August 2000, but a last minute revision by security agencies in Vietnam saw the project site moved to Central Luzon in the Philippines.

The literature

Briscoe and Brown (1998) observe that, to date, there has been limited experience with polarimetric radar in agricultural applications, and that multi-waveband research results are also limited, compared to work done with single wavebands. They also note that comparatively little work has been done on tropical agriculture.

A large amount of the foundation work in radar remote sensing, beginning in the late 1970s was done by Ulaby and various collaborators in the US, and by Hoekman and Boumann in the Netherlands, using ground-based scatterometers and airborne instruments. Ulaby has continued to be at the forefront of research in SAR as polarimetric radars such as AirSAR have become available. The Shuttle Imaging Radar Mission (SIR-C) allowed polarimetric data to be collected from space in X, C and L band – for example

[2] Australian Centre for International Agricultural Research.

Soares' data was obtained from SIR-C. Single waveband, single polarisation radars on Radarsat (C_{hh}), ERS-1 and 2 (C_{vv}) and JERS-1 (L_{hh}) have widened the availability of data for agricultural applications. However, the inherent limitations of the technology have meant that the main avenues for adequate crop classification lie in 1) multi-temporal analysis and/or 2) combination with optical and infrared remote sensed data.

Much early work was done using K- and X-band radars, which are more sensitive to the surface roughness of crops, but many of the airborne instruments had comparatively coarse resolution (scale = 1:400,000). Bush and Ulaby (1978) found that X_{vv} (_=2cm) provided the best discrimination of corn, soybean, wheat, milo and alfalfa and achieved a 90% classification accuracy. Haralick (1970) found that HH and HV images enhanced the identification of sugar beet, corn, grain sorghum, wheat and alfalfa at different cropping densities. Briscoe and Protz (1980) achieved a 90% correct classification of corn using simultaneous X and L band radar in one pass.

Much of the early work also investigated variations in response with incidence angle, leading to the development of the cloud models and their successors (Attema and Ulaby, 1978).

Airborne X-band radar was used to provide complete land-use and land cover maps for the whole of Nigeria (Trevett, 1986). McDonald and Indradi (1991) were able to classify mixed forest, old and new rubber, oil palm, coconut, cassava, rice and maize using X_{hh} with a 6X6m pixel resolution and noted that stereoscopic SAR imagery could generate land-use maps five times faster than form 1:40,000 aerial photography.

C-band was found to be better at separating lush crops such as Soya bean from corn (Mehta, 1983). Le Toan (1989) recommended the use of polarisation ratio (hh/vv) to identify grain crops as the vertical polarisation is attenuated more strongly than the horizontal, which penetrates the canopy and responds to soil moisture. Briscoe (1992) found that HV returns considerably aided crop discrimination in all wavebands.

As noted earlier, there has been conflicting evidence in literature, mainly concerning cereals. In multi-temporal analysis, changes in characteristic signature are used to distinguish crop types: for example. Broad-leaved crops, such as sugar beet and potato attain full vegetative cover early and the backscatter reaches a plateau and does not change over the remainder of the season (Bouman, 1999), but that of wheat decreases as vegetative growth occurs. In contrast the backscatter response of rice appears to increase with vegetative growth, and Le Toan (1997) showed that both $_{hh}$ and $_{vv}$ backscatter increased at early growth stages, but that as full canopy cover is developed the proportion of $_{vv}$ decreases whilst $_{hh}$ increases. Polarisation ratio was again found to be a good discriminant of growth stage.

Rosenqvist (1998) showed a strong correlation between L_{hh} backscatter (JERS-1) with plant growth in paddy rice. He observed strong Bragg scattering from fields in Japan, where rows were perpendicular to the incident beam and inter-row and within-row plant spacing was precise and typically 30cm. By contrast Durden (1995) observed little

attenuation of L_{vv} or L_{hh} in rice. Durden (1995) and Le Toan (1997) both observed that direct volume scattering from C_{vv} was minimal in rice, and so the reflection of C_{vv} is largely due to water surface, canopy interaction, unlike in the case of wheat and barley (Bouman, 1999).

Multitemporal analysis can be improved if the start and end of crop seasons are known (Le Toan, 1989 *et seq*.). Markers for the start of a rice season are the transition from ponding to transplanting, and similar markers can be found in pastures, which are cut for hay. Foody (1989) showed that classification accuracy rose from 55% at the first pass to 90% after four passes. Two-date polarimetric datasets (summer and winter) proved better at discriminating forest types in northern Canada (Ranson and Sun, 1993) at 81.1% compared to 66% for the summer data alone.

A change index is usually used to evaluate differences in crop condition between successive passes of the same sensor (Ribbes and Le Toan, 1999). Liew at al (1998) define a change class as follows:

$$\int = \Delta\sigma \circ (dB) = 20\log_{10}\left(\frac{DN1}{DN2}\right)$$

where:
DN1 = pixel digital number of the first of two consecutive pairs of images
DN2 = pixel digital number of the second image in a pair.

In a study of farming systems in the Mekong Delta, pixels were classified as constant if change was less than ±3dB. 9 thematic classes were merged from 243 unique change classes over 7 satellite passes. Considerable ambiguity exists in the resulting classifications over the period May to December.

Verhoeven *et al*. (2000) notes that a multi-temporal filter for speckle is required with consecutive images in order to preserve image precision. In trying to apply Le Toan's 3dB change detection threshold, they observe that it works well for large, flat, homogenous areas, where rice is planted at the same growth stage, but that this is not the case in most SE Asian countries. They are attempting to address the crop seasonality and number of crops per year by adding a data bas of local statistics, high-resolution aerial photography and additional conventional remote sensing data, combined through the use of GIS.

In preparation for the PACRIM AirSAR mission, a matrix of expected radar responses of different crop and ground conditions was developed for all combinations of waveband and polarization, based on a simple understanding of radar-ground-vegetation interactions and some simple modelling using 1 and 2-layer cloud models (in Fortran and Excel). This indicates that most expected ground conditions could be determined with combinations of C_{vv}, C_{hh}, L_{vv}, C_{hv} and L_{hh} signals.

Ground-truth Fieldwork

Two sites were identified in Districts 1 and 4 of the Upper Pampanga Region Integrated Irrigation System (UPRIIS). Rice planting in the Philippines historically follows a stricter seasonal pattern than in neighbouring countries, but District 4 had been experimenting with further intensification of rice cropping, and significant areas of planting were scheduled for the agreed PACRIM flight dates in September 2000.

Figure 1 a) Location map for ground truth work on rice mapping in the Philippines b) detail of the survey area in District 4 at Gapan (vector polygons of survey area shown).

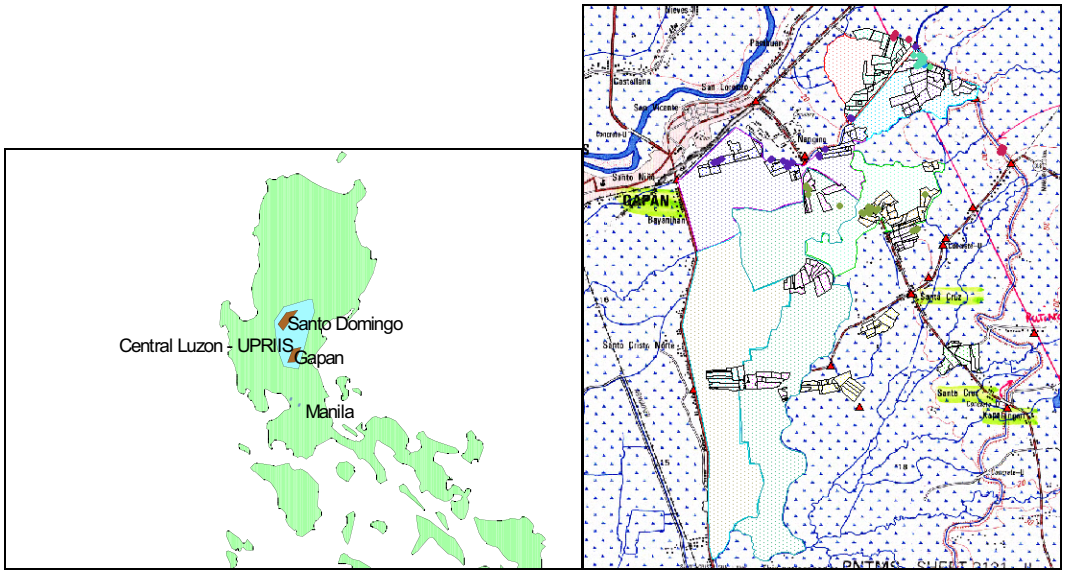

A reconnaissance survey in July revealed that the full range of rice growth stages could be expected to be identified in District 1 (known here as Santo Domingo) and District 4 (known here as Gapan) at the time of data acquisition. On September 25, there were predominantly mid-late growth stages and harvested fields in Santo Domingo and predominantly land preparation, transplanting, early and maturing growth stages in Gapan. The two sample sites are approximately 40km apart.

Field survey was conducted by 45 field workers, over three days from 25-27 September, 2000. Surveyors in Santo Domingo were hired from the National Irrigation Administration (NIA) field staff and those in Gapan were sourced from NIA field and operations staff and from young graduates. A total of 450 ha covering more than 400 plots were surveyed over the three days at the two sites.

Field sites were identified over the previous three weeks, using a hand-held GPS, to locate plots and blocks at appropriate growth stages. 1:50:000 scale topo-maps were

scanned and incorporated into a GIS, to provide a base layer. A complete set of aerial photographs at 1:38000 scale were purchased from the National Land Administration in Manila, and were used in conjunction with cadastral maps sourced from NIA, and the local administrations, to mark out and identify plot owners.

Two trainings were held for field staff, to confirm accurate recognition of crop growth stage and other important crop parameters. Survey indexes were used to identify cadastral plots by owner name and number. In Santo Domingo, farmers typically own a long rectangular strip, known as a "Banoz", 1 to 2 plots wide, up to more than 20 plots long. In Gapan, the plot arrangement is more variable. Where crop growth stage or condition was not homogenous on survey day, the field measured plot boundaries and annotated hand-drawn maps on the survey forms.

The following typical ground conditions were sampled:

1) Bare soil – dry
2) Ploughed land
3) Flooded land, prior to transplanting or direct seeding.
4) Newly transplanted fields
5) Nursery plots
6) Rice at emergence
7) Rice at tillering
8) Rice at head formation
9) Rice at maturity
10) Newly harvested rice (tall stubble)
11) Short stubble
12) Bare soil after burning stubble.

In practice, crop growth stages were further differentiated at three stages of vegetative growth prior to heading and also at flowering and two grain-fill stages (milky grain and dough grain). Fallow or weed covered paddocks were also sampled, plus a few non-rice crops, where they could be found.

Figure 2 Rice growth stages

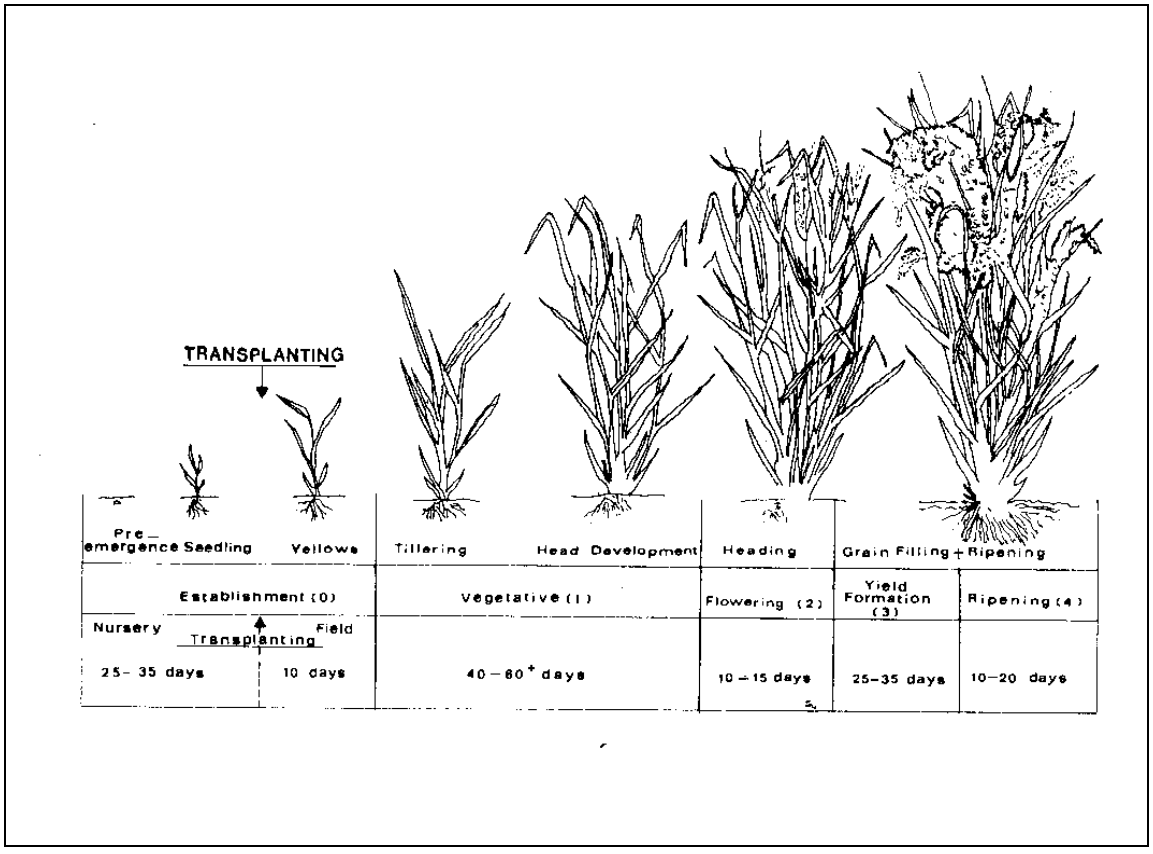

A number of soil and crop characteristics were also collected including:

1) Soil condition – bare, ploughed, levelled, ponded, cropped, stubble, burnt, and fallow.
   - Sample soil moisture content using Time Domain Reflectometry
   - Measurement of soil surface roughness, using a profile meter and a white board, with registration points. Photographs were taken of soil surface profile against the white board.
2) Crop information for rice:
   - Variety
   - Transplanted or direct sown (T/DS)
   - If transplanted – row orientation in degrees using a compass.
   - Crop growth stage
   - Number of plants per square meter: plant spacing if transplanted
   - Number of tillers per plant based on sample in $1m^2$ quadrats.
   - Average water depth
   - Sample total biomass per square meter for some plots using a modified pasture plate meter. Crop cuts were not possible.
3) Field features
   - Proximity to large banks, roads, channels
   - Field bank height

During crop growth stage sampling, sample sets of field were sampled for biomass, using a modified pasture plate meter. Approximately fifteen samples were taken per field to get an average value for the location. The pasture plate meter[3] readings should be calibrated against crop cut data (Earle and McGovern, 1979) to provide estimates of biomass. Since crop cuts have not been done, this data gives a measure of relative biomass only.

Since the soil profile meters got detained in customs, soil roughness estimates were made in the same way as crop roughness measurements. A large white board, with at least 8 registration points was placed on the soil surface, and photographs were taken at a shallow angle to present an outline that could subsequently be digitized. Long-scale macro-roughness was not measured.

Soil moisture data was collected at a test site one day before the overflight, and 12 "dry" blocks were sampled on the flight day in Santo Domingo only. One third of these locations had soil moisture conditions close to saturation. The location of the soil moisture samples using TDR (surface 20 cm only) was recorded using GPS. Typically 10-15 samples were taken in one plot.

[3] A pasture plate meter measures the extent of compression of vegetation when a 1 m^2 plate is allowed to fall on the crop surface. It is widely used in Australia for pasture and has also been used for wheat. Calibrations are required for different growth stages, due to the lignification of stems in later growth stages.

Field data preparation

All field data was transcribed to spreadsheet, and tables of crop and ground conditions were prepared so that they could be exported to GIS. The GIS is based on scanned topo-maps, projected in UTM (Clarke 1866 spheroid (Luzon datum). All GPS data for registration points (cross roads and junctions, channel crossings, and major irrigation structures) were imported and corrected to the Luzon datum. We observe a remarkable correspondence between map and GPS position, with generally less than 5m error in location, which is surprising for 1:50,000 scale maps, where 1 mm error in digitising translates to 50 m in the real world.

Diapositive airphotos were also obtained in the Manila from NAMRIA, and these were scanned at high resolution (9600 dpi) to obtain maximum resolution, since the scale was coarser than ideal for identifying field boundaries. Nevertheless, each individual plot boundary is visible in the GIS, providing TIFF files are used rather than compressed formats. The airphotos were registered to the base-maps and then mosaicked. Resampling in mosaicking reduces image precision and individual air photos were used to locate field plots.

Figure 3 Schematic summary of ground truth data preparation for image processing

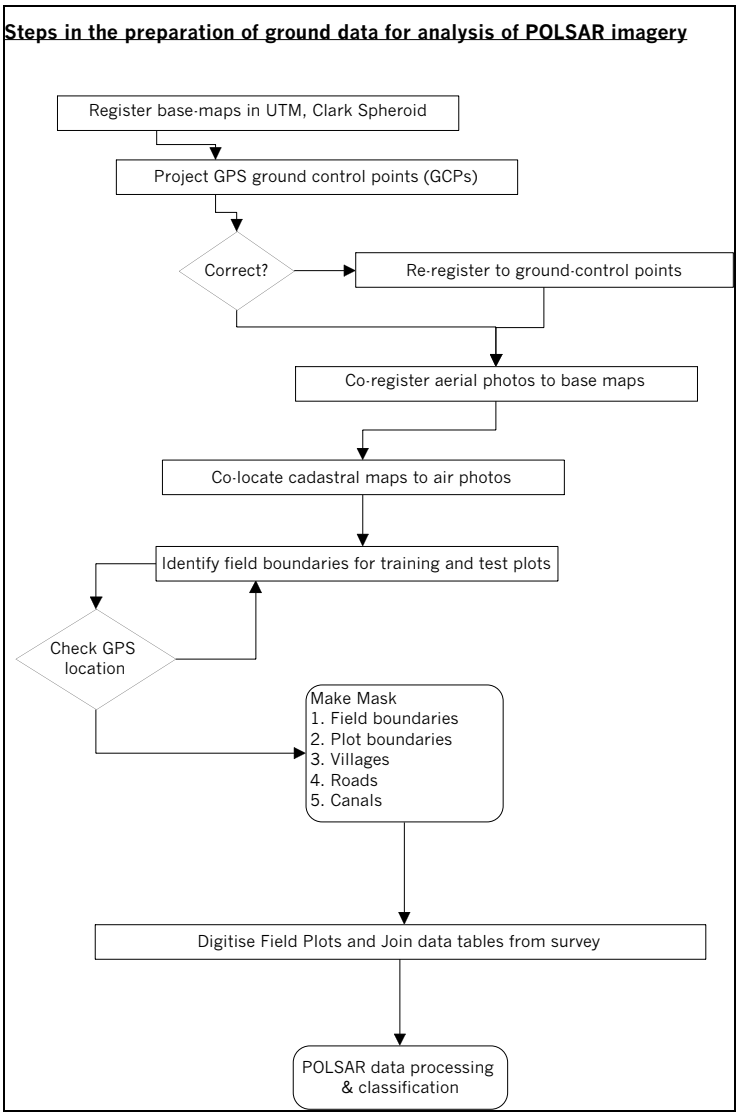

The cadastral maps are indexed by name, plot number, and area with plot numbers used as indexes for field data collection. The cadastral maps are often not topologically accurate, and require some interpolation when digitizing. In an ideal world, each field boundary would have been determined using DGPS, since GPS location accuracy is insufficient for mapping plot boundaries at this resolution. However, most plots are unambiguous especially when they form contiguous blocks at one growth stage. Sketch maps made at sampling time also improve plot identification. There is some uncertainty when sample blocks contain a number of growth stages, particularly when these are patchy. It was observed that plot identification could be aided by reference to the AirSAR images, but this defeats the point of ground truthing and the temptation was overcome!

There is an interesting conundrum here in subsequent ground truth accuracy and tests of classification accuracy. This will be explored later, if there are any obvious errors in the ground truth data set, either by correcting training data to the AirSAR image, or by discarding them.

All ground truth polygon files are joined to their respective field data tables, and then sorted by ground truth class. Initially these classes are based on crop growth stage alone. There are many possible enhancements, the most obvious being the distinction between crop growth stages with ponded or dry soil conditions under the canopy. This is most likely to make a difference to the observed backscatter, since the proportion of double bounce scattering in C and L band should increase considerably if reflected off a water surface below the crop canopy.

Each class is exported as one shapefile, for inclusion in ENVI and conversion to raster format (ROI – region of interest) for image classification. Each class is divided in two to provide training and test areas. This is a time consuming process.

Soil and crop surface roughness was analysed by digitizing the photographs taken of the crop or soil surface set against the white boards used in the field. At least four registration points have to be visible in the photograph to obtain good results. Digitising soil surface roughness is straightforward, but a number of trials were required for the crop canopy cover. The initial calculations of RMS roughness height proved to be very sensitive to the number of digitizing points taken, and it was found that a minimum of some 150 points in a 2m segment is required for adequate comparison.

One pasture plate meter was left in the Philippines with the International Rice Research Institute in Los Banos, in the hope of being able to obtain some crop cut data that would correspond to readings taken at different growth stages, using similar varieties.

Image Processing

All images are analysed in dB form, with correction to ground range. Preservation of radiometric characteristics was checked for pixels at individual locations and for ROIs covering the same target area in slant range and ground range images, prior to and also after image registration. Differences in average backscatter coefficient for all wavebands was found to be less than 0.17 dB for selected regions, which is very encouraging. Individual values at one location varied by as much as 1 dB due to some pixel shift.

The overall image analysis pathway is summarized in Figure 4, although in practice, this has turned out to require more steps and detail in the intermediate stages.

Figure 4 Initial image processing strategy to determine classification accuracy.

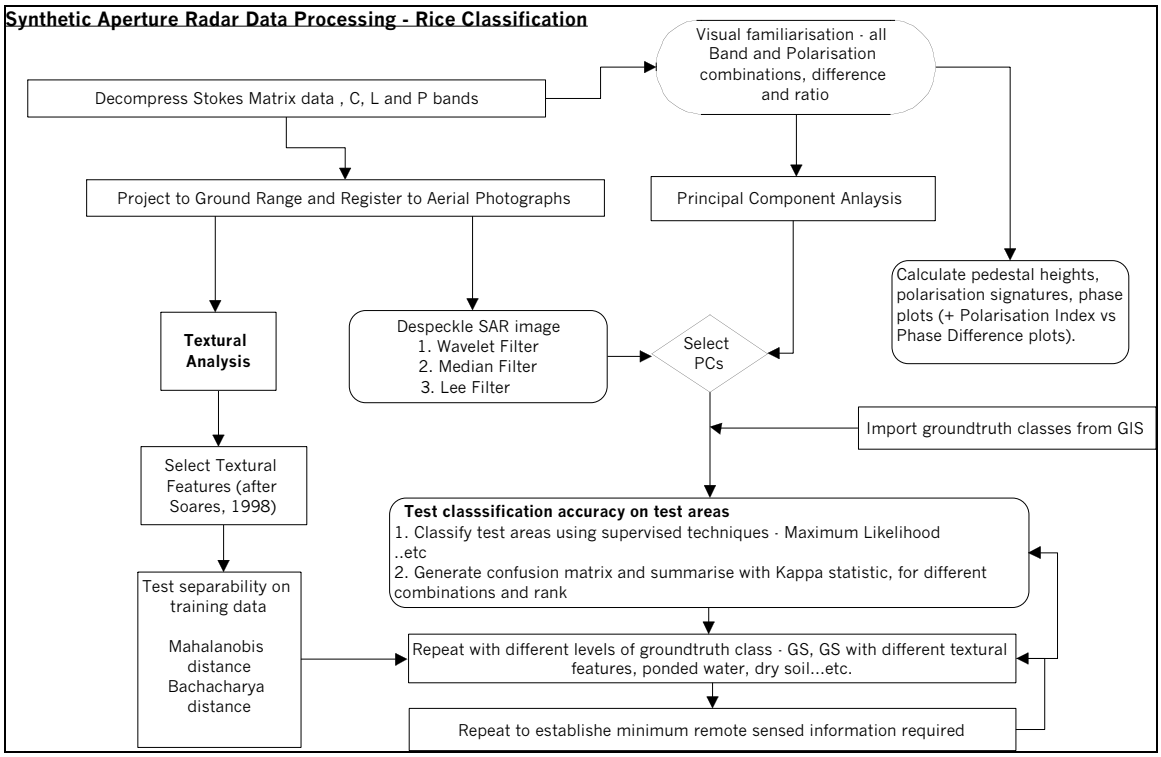

Principle Component Analysis (PCA) was performed separately for Gapan and Santo Domingo images, using sigma values of backscatter coefficient in the slant range. We observe different results reflecting predominantly early and late growth stages respectively (see Table 1), where C_{vv} and C_{hv} are interchanged. C_{vv} is better correlated to early vegetative stages, whereas C_{hv} represents increased volumetric scattering from the crop canopy after grain formation . ENVI calculates C_{hh} as the fifth significant principal component, but this should not be possible, since it is the first PC.

	Gapan		**Santo Domingo**	
Principal Component	Band and polarisation	Eigen Value	Band and polarisation	Eigen Value
1	C_{hh}	0.623	C_{hh}	0.594
2	C_{vv}	0.569	C_{hv}	0.666
3	L_{TP}	0.558	L_{TP}	0.305
4	L_{vv}	0.499	L_{vv}	0.568
5	C_{hv}	0.349	C_{hh}	0.462
6	L_{hh}	0.743	L_{hh}	0.737
7	P_{vv}	0.791	-	

Table 1 Principle components of AirSAR images for Gapan and Santo Domingo

More than 60% of the response is accounted for by the first two PCs. P_{vv} may be significant in Gapan due to greater amounts of tree cover and settlement than in Santo Domingo which is more open.

It should be possible to calculate PCs for targets in both images, but both images need to be co-registered first. It is desirable to look at the relative importance of other measures, such as phase difference, bounce classification, pedestal height and band ratio. Pedestal heights for C, L and P band have the same value scale as sigma 0 backscatter coefficient and can therefore be compared and indeed are higher ranked that waveband combinations. However, it is not clear what this information means in practice.

All subsequent image processing was conducted on the Gapan data set only, but will be repeated for Santo Domingo and for a combined data set in the future.

In order to test image classification using polarimetric data only, the images were converted to ground range and registered and processed as follows:

1. Image registration
    a. subset polarimetric image to aerial photographs of survey area (one only for Gapan), using cubic convolution, with third degree polynomial nearest neighbour resampling.
    b. image to map registration is preferred to be able to select pixel size similar to original image (3.93 by 3.93 m pixels). Image to image registration in ENVI allows no control of pixel size and results in enormous and unwieldy images.
2. Frost filtering (3x3) prior to conventional classification.
3. Classification measures
    a. Importation of shapefile ground truth classes.
    b. Conversion of shapefile classes to two sets of ROIs – training and test locations.
    c. Supervised classification
        i. Maximum Likelihood and ……compare
    d. Analysis of classification accuracy using confusion matrix.

In practice, a secondary image registration is required, as image to map registration resulted in local distortions over certain parts of the ground truth areas, by up to 20m. The re-registration was done on the previously registered image, by refining ground control points taken from the vector layer of all ground truth data. Second-order polynomial, nearest neighbour resampling with cubic convolution was used to minimize further warping.

Textural analysis is being undertaken using unfiltered ground-range images, using the technique outlined by Soares et al (1998), and using IDL code kindly provided by Soares and Renno (2001).

RESULTS

Soil moisture in sampled plots in Santo Domingo was high across a range of growth stages, even during maturity and harvest, as shown in Table 2. Volumetric moisture contents of 50% or more are close to saturation, even though there is no water ponded on the surface. From observation, this would be typically the case at Gapan also. Signal attenuation should therefore be high on high moisture content but unponded soils, and immediately ponding occurs, the return signal strength should increase due to double bounce scattering in both C-band at early growth stages, L band in mid and late growth stages, and P-Band at late growth stages.

LDMK	Plot #	IA	GS	PPM cm	VMC av %
1	654	VEGA COSTRA	ET2	28	45.25
2	221	VEGA COSTRA	HH-FL	83	47.50
3	211	MAMBARAO	FL	44	34.15
4	42	MAMBARAO	FL	54	38.25
5	11	MAMBARAO	FL	55	56.40
6	355	VEGA COSTRA	MG	70	52.20
7	411	NALBUGAN F2-1	MG	70	54.30
8	232	VEGA COSTRA	MG-DG	45	57.10
9	414	MAMBARAO	DG	67	27.65
10	533	MAMBARAO	DG	87	52.65
11	413	VEGA COSTRA	HVST	91	54.20

Table 2 Summary of TDR measured average plot soil moisture content at Santo Domingo.

RMS roughness of the crop appears to increase steadily with growth stage, as shown in Figure 5 below. In this areas rice ears are removed at the top of the stem, rather than the stem being cut close to the ground. This leaves much upright, lignified vegetation in the field immediately after harvest, which is eventually burnt off or grazed. The points shown on the graph have been derived from 32 plots in Gapan and represent average times to the following ground conditions 1) Ponded, ploughed land, prepared for transplanting or sowing (-20); 2) Mid-vegetative stage, about PI; 3) Flowering; 4) Harvest; 5) Standing stubble after harvest. The increasing brightness of C –band reflection at later growth stages is clearly partly attributable to this.

Figure 5 Relationship between RMS surface roughness and crop development, for field plots in Gapan.

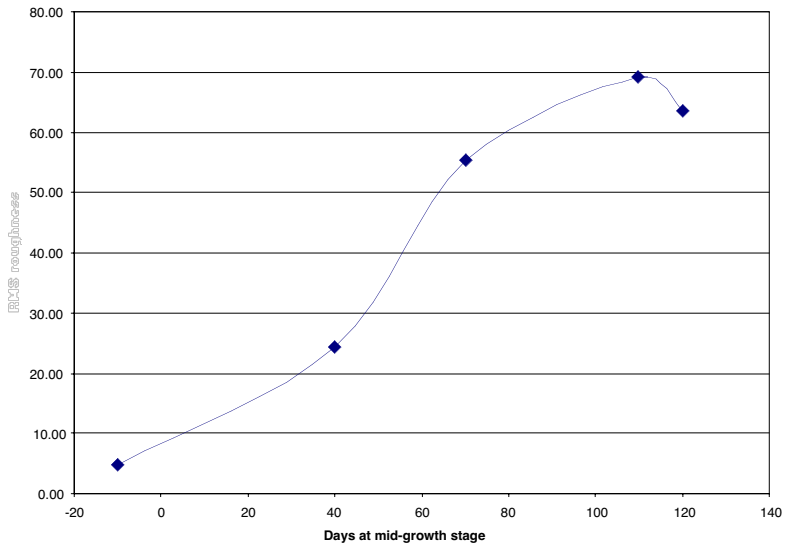

Class average values of dB backscatter have been calculated for the training data set (16 of 17 classes) for Gapan and those for the 7 principal components identified earlier have been plotted in Figure 6.

The crop season starts at transplanting, which is conventionally given the day value zero. For reference, the backscatters for Fishponds are given on the left of the plot and those for bare dry soil after harvest and burning, on the right. Backscatter for fishponds can be differentiated from ponded paddies by the extent of double bounce returns and from the pond embankments and the resulting higher power return. There is no data for the very early vegetative growth stages

Backscatter can be seen to increase with vegetative development, in both L and P bands, although a short-term dip of 4 dB is apparent at flowering. The ratios of C_{hh} and C_{hv} to Cvv should give differentiation of later growth stages. The sharp but temporary peak at heading may be due to a large number of vertical stems acting as small antennae, increasing the proportion of double bounce returns before the florets spread. This is characteristic even of the P-band, which is surprising.

Observing the data indicates that as the rice crop develops, its radiometric properties increasingly resemble that of a fishpond, and indeed this is the classification that is seen with simple minimum distance methods, probably with an insufficiently well-specified set of parameters.

Figure 7 Backscatter returns for the main principle component wavebands – Gapan ground truth training dataset.

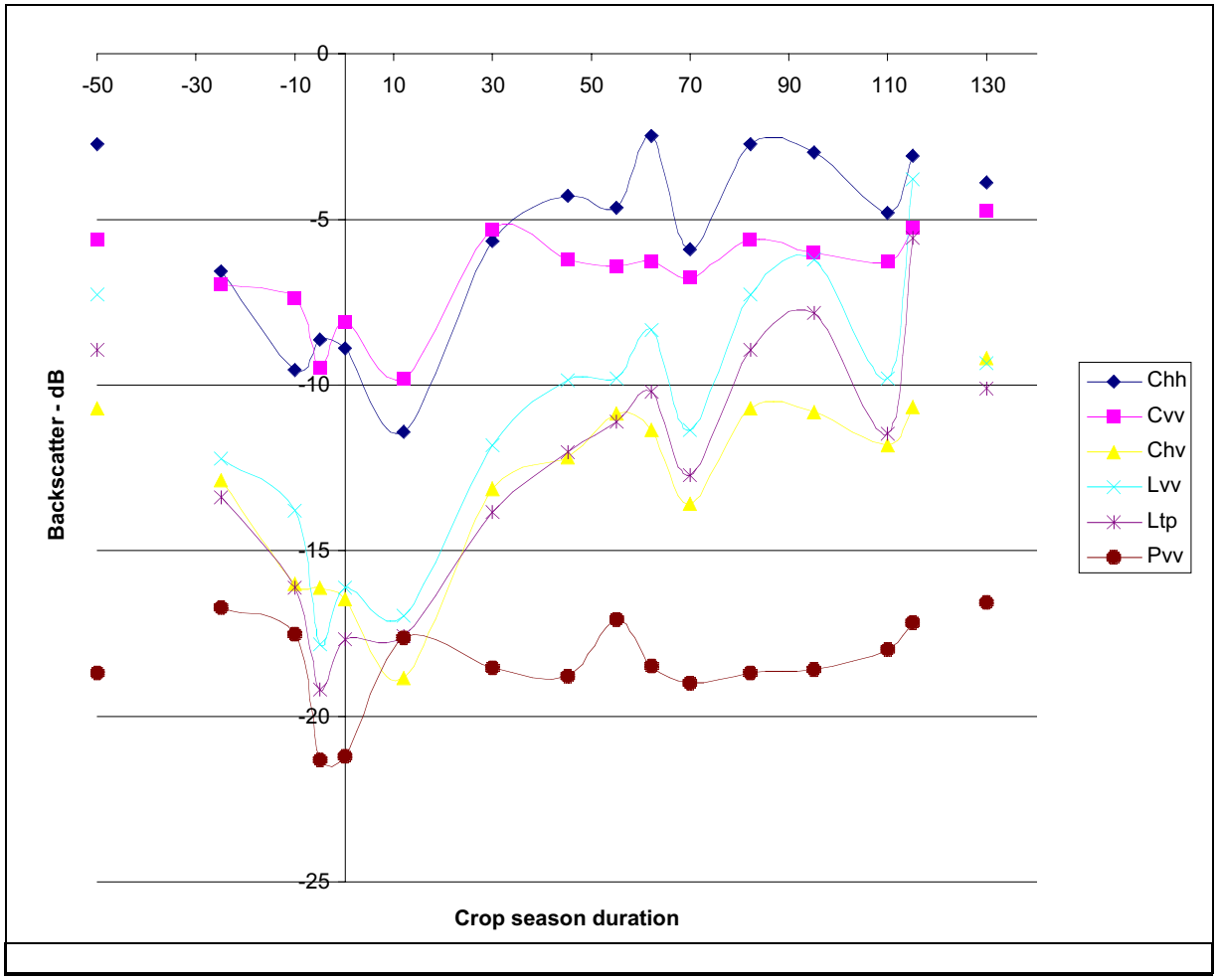

FP PP N TT EM EV2 PI BT HH FL MG DG HV X BD

Key

FP	Fish Pond	HH	Heading
PP	Ploughed & ponded	FL	Flowering
N	Nursery beds	MG	Milky Grain Stage
TT	Transplanting	DG	Dough Grain Stage
EM	Emergence (direct seeded)	HV	Harvest ready
EV2	Early vegetative stage 2	X	Cut
PI	Panicle Initiation	BD	Bare dry soil
BT	Booting		

The dip in C-band and L-band return signal at flowering is harder to explain, and effects of canopy closure do not convincingly explain the attenuation, where it is conceivable that there is more direct reflection from the canopy surface, with a slightly higher dielectric and “apparently” smoother surface.

Supervised Classification

The primary objective of this initial work was to evaluate the classification accuracy of POLSAR, using the ground truth data divided into training and test data sets. At the time of writing, this objective has not been met.

The preceding discussion indicates good possibilities for acceptable classification and indeed, supervised classification based on manually entered ROIs for known vegetation classes, gave visually impressive results.

At the moment, there appear to be statistical problems with some of the field data, with the result that it has not been possible to calculate a full set of Class statistics. One set of ROIs causes the ENVI software to expire, but even when left out of the set, class separability cannot be properly calculated and Maximum Likelihood Classification is not possible. Classification by Mahalanobis Distance results in a set of rule images that, when converted to a three-band rule image, results in something that looks acceptable, as shown in Figure 8. However, the classification image itself is monotone and cannot be used to determine a confusion matrix using the test ROIs.

Figure 8 Rule image for a subset of Gapan, using the Mahalanobis distance classifier.

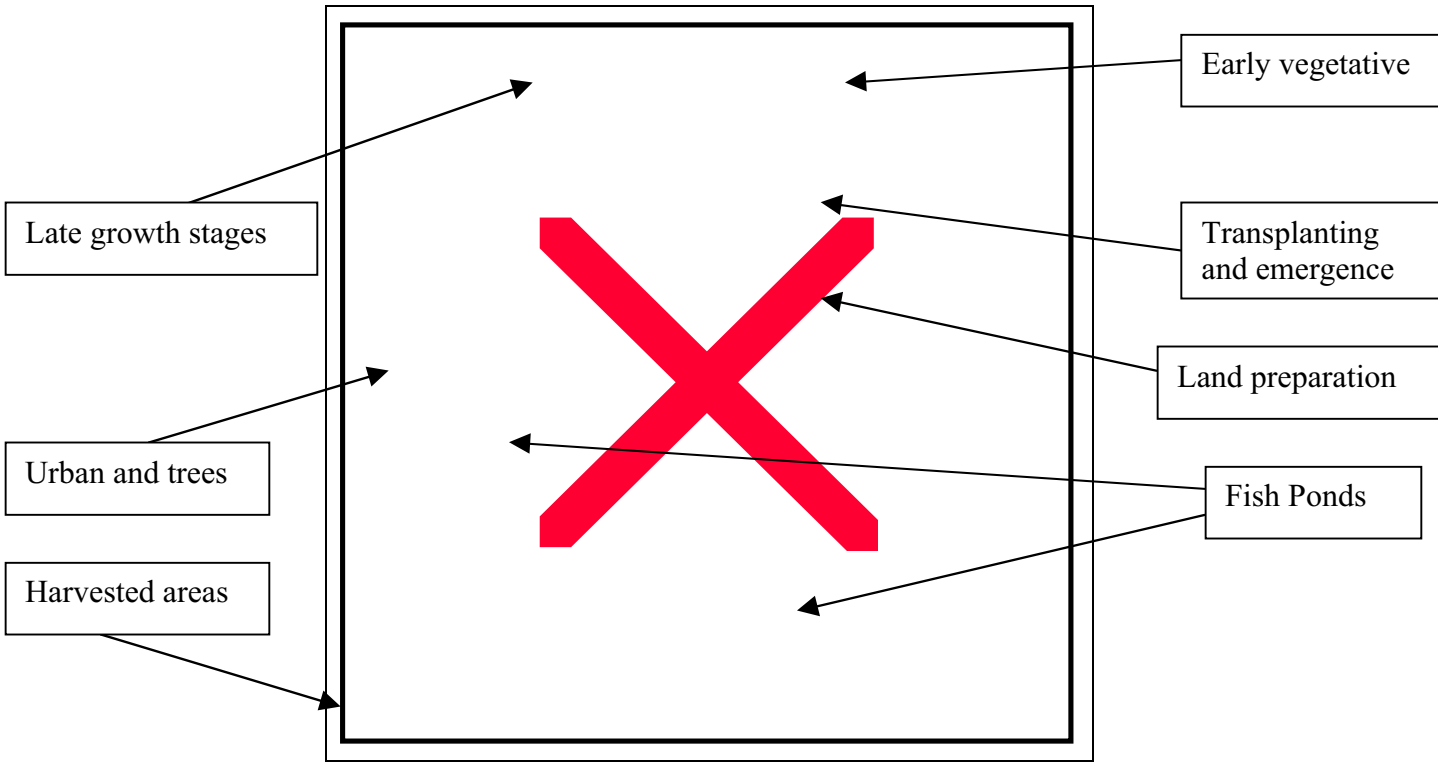

It is clear that the number of classes to be determined should be reduced to a more separable set, and that urban and forest need to be either masked or added as separate classes. It is also clear from overlaying the vector data that a small proportion of the

training and test sets need to be adjusted as their boundaries clearly do not match what is seen in the radar image. Such ambiguous polygons can be eliminated or corrected, but this is better done after establishing a baseline with the data as collected. There are many class permutations beyond simply the crop growth stage, such as the presence or absence of ponded water, crop row orientation at young growth stages (affecting surface roughness and Bragg Scattering). Further understanding and investigation is required to complete a formal classification analysis and then refine it.

Acknowledgements

A great deal of help, enthusiasm and hard work was provided by the staff of the Philippines National Irrigation Administration in Central Luzon, especially the operations engineer for District 1, Engineer Willy Ramos, the manager for District 4, Ray Puno and the field staff and their relatives who conducted the ground survey.

The author would like to thank NASA JPL, Ellen O'Leary, Tony Milne (UNSW) and Ian Tapley (CSIRO), for providing the opportunity to join PACRIM 2000 and then having the flexibility to cope with last minute programme changes.

Cress Savige, of Melbourne University, has put in a great deal of time in the collation and anlaysis of the field data.

ACIAR Project 9834 "System Wide Water Management in Public Irrigation Systems in Vietnam", provided the funding to undertake this study, in support of decision support system development in irrigation in general.

References

Attema, E. and Ulaby, F., 1978. Vegetation modelled as a water cloud. Radio Science, 13: 357-364.

Boumann, B., 1988. Microwave backscatter from Beets, Peas and Potatoes throughout the growing season, Spectral Signatures of Objects in Remote Sensing, Aussois, France, pp. 25-30.

Brisco, B. and Brown, R., 1995. Multidate SAR/TM synergism for crop classification in western Canada. Photogrammetric Engineering and Remote Sensing, 61(8): 1009-1014.

Brisco, B. and Brown, R., 1998. Agricultural Applications with Radar. In: F. Henderson and A. Lewis (Editors), Principles and Applications of Imaging Radar, Manual of Remote Sensing. John Wiley and Sons Inc., New York, pp. 381-400.

Brisco, B., Brown, R., Koehler, J., Sofko, G. and MJ, M., 1990. The diurnal pattern of wheat radar backscatter. Remote Sensing of Environment, 34: 37-47.

Brisco, B. and Protz, R., 1980. Corn field identification accuracy using airborne radar imagery. Canadian Journal of Remote Sensing, 6(1): 15-24.

Briscoe, B., Brown, R., Gairns, J. and Snider, B., 1992. Temporal ground-based scatterometer observations of crops in western Canada. Canadian Journal of Remote Sensing, 18(1): 14-21.

Dong, Y. and Forster, B., 1996. Understanding Partial Polarisation in Polarimetric SAR data. Int. J. Remote Sensing, 17(12): 2467.

Dong, Y., Forster, B., Milne, A. and GA, M., 1998. Speckle suppression using recursive wavelet transforms. International Journal of Remote Sensing., 19(2): 317-330.

Dong, Y., Richards, J. and Cashman, J., 1995. A model of volume attenuation and backscattering by foliage at L- and P- bands. International Journal of Remote Sensing, 16(7): 1231-1247.

Dubois, P.C., van Zyl, J. and Engman, T., 1995. Measuring soil moisture with imaging radars. IEEE Transactions on Geoscience and Remote Sensing, 33(4): 915-926.

Durden, S., Morrissey, L.A. and Livingston, G., 1995. Microwave Backscatter and Attenuation Dependence On Leaf-Area Index for Flooded Rice Fields. IEEE Transactions On Geoscience And Remote Sensing, 33(3): 807-810.

ed. Henderson, F. and Lewis, A., 1989. The Manual of Remote Sensing:, 2. John Wiley and Sons, New York, 866 pp.

Earle DF and McGovern AA, 1979. Evaluation and calibration of an automated rising plate meter for estimating dry matter yield of Pasture. Australian Journal of Experimental Agriculture and Animal Husbandry, 119: 337-343

FAO, 1993. Use of Remote Sensing Techniques in Irrigation and Drainage. In: A. Vidal and J. Sagardoy (Editors), Use of Remote Sensing Techniques in Irrigation and Drainage. FAO Water Reports. FAO, Rome, pp. 202.

FAO 1996

Foody, G., Curran, P., Groom, G. and Munro, D., 1989. Multi-temporal airborne synthetic aperture radar data for crop classification. Geocarto International, 3: 19-29.

Haralick, R., 1979. Statistical and Structural Approaches to Texture. Proceedings IEEE, 67(5): 786-804.

Haralick, R., Shanmugan, K. and Dinstein, I., 1970. Using radar imagery for crop discrimination- a statistical and conditional probability study. Remote Sensing of Environment, 1: 131-132.

Le Toan, T., Laur, H., Mougin, E. and Lopes, A., 1989. Multi-temporal and Dual-Polarisation Observations of Agricultural Vegetation Covers by X-band SAR images. IEEE Transactions on GeoScience and Remote Sensing, 27(6): 709-718.

Le Toan, T. et al., 1997. Rice Crop Mapping and Monitoring Using ERS-1 Data Based on Experiment and Modelling Results. IEEE Transactions on Geoscience and Remote Sensing, 35(1): 41-56.

Leckie, D., 1990. Synergism of Synthetic Aperture Radar and Visible/Infrared Data for Forest type discrimination. Photogrammetric Engineering and Remote Sensing, 56(9): 1237-1246.

Liew, S. et al., 1998. Delineation of Rice Cropping Systems in the Mekong River Delta using Multi-temporal ERS Synthetic Aperture Radar. Centre for Remote Imaging, Sensing and Processing, National University of Singapore.

MacDonald, B. and Indradi, 1991. Land Use Interpretation of STAR-1 synthetic aperture radar data in Indonesia: a practical example., 14th Canadian Symposium on Remote Sensing, Calgary, Alberta, pp. 337-341.

Mehta, N., 1983. Crop identification with airborne scatterometers, International Geoscience and Remote Sensing Symposium Proceedings, San Fransisco.

Ranson, K. and G, S., 1993. Northern Forest Classification Using Temporal Multifrequency and Multipolarimetric SAR Images. Remote Sensing of the Environment, 47: 142-153.

Ribbes, F. and Le Toan, T., 1999. Rice Field Mapping and Monitoring with Radarsat data. Int. J. Remote Sensing, 20(4): 745-765.

Saktivadivel, R., 1999. Performance Evaluation of the Bhakra Irrigation System, India, using Remote Sensing and GIS techniques. 28, IWMI, Colombo.

Soares, J., Renno, C., Formaggio, A., Yanasse, C.d.C. and Frery, A., 1997. An investigation of the selection for texture features for crop discrimination using SAR imagery. Remote Sensing of the Environment, 59: 234-247.

Toure, A., Thompson, K., Edwards, G., Brown, R. and Briscoe, B., 1994. Adaptation of MIMICS backscattering model to the agricultural context: wheat and canola at L and C bands. IEEE Trans. on Geosciences and Remote Sensing.

Trevett, J., 1986. Imaging Radar for Resource Surveys. Chapman and Hall, London, 313 pp.

Verhoeven, R., van Leeuwen, H. and van Valkengoed, E., 2000. Monitoring rain-fed and irrigated rice in South East Asia using radar remote sensing, ? ?, ?

Vidal, A., 2000. Remote Sensing and Geographic Information Systems in Irrigation and Drainage. ICID Handbooks. ICID Central Office, Delhi, 126 pp.